long bones and ribs. Males with 3M syndrome occasionally have hypogonadism and hypospadias (1–9). However, intelligence is unaffected and karyotype is normal on conventional chromosome analysis.

In patients with 3M syndrome, disease-causing mutations have been identified in the cullin 7 (*CUL7*, MIM *609577) and obscurin-like 1 (*OBSL1*, MIM *610991) genes (7–9). Mutations of *CUL7* are the major cause of 3M syndrome, accounting for 80% of previously reported cases, whereas *OBSL1* accounts for 20% of cases (8, 10).

Uniparental disomy (UPD) is the transmission pattern of either two copies of the identical chromosome (uniparental isodisomy; iUPD) or of both homologous chromosomes (uniparental heterodisomy; hUPD) from one parent with no contribution from the other parent (11). Phenotypes that are clinically associated with paternal UPD of chromosome 6 (patUPD6) and genomic imprinting have been established, but because of the rarity of maternal UPD of chromosome 6 (matUPD6), clinical features have not yet been established. Here, we report a patient with a homozygous mutation in *CUL7* due to a maternal iUPD of chromosome 6 (mat-iUPD6).

Materials and methods

Clinical report

A Japanese male patient with 3M syndrome was examined in this study. The patient was delivered by caesarean section at 36 weeks of gestation without a family history of 3M syndrome (Fig. 1a). His birth weight was 1000 g (−4.8 SD), length 33.0 cm (−6.8 SD), head circumference 30.2 cm (−1.5 SD), and Apgar score 7/9. Feeding difficulty was noted during the neonatal period. He remained in a neonatal intensive care unit for 2 months and was referred to our group because of developmental delay and muscle hypotonia at 4 months. The patient displayed anomalies including hypospadias, inguinal hernia, hydrocele testis, inverted triangular gloomy face, malar hypoplasia, long eyelashes, epicanthal folds, short nose, anteverted nares, full lips, long philtrum, pointed chin, short chest, grooved lower anterior thorax, hypermobility of joints, and slender long bones (Fig. 1a,b). Mild ventricular enlargement was observed by neuroradiological studies. His growth was severely retarded.

At 2 years 9 months, his height, weight, and head circumference were 69.3 cm (−4.6 SD), 6.8 kg (−6.7 SD), and 48 cm (−1.2 SD), respectively. His head size was disproportionately large compared to his height. Thus the patient was diagnosed as suffering from 3M syndrome. He could understand simple sentences, but could not speak nor sit alone. Partial growth hormone (GH) deficiency was noted. GH replacement therapy was started from 2 years. GH was effective without side effects. At 5 years, his height and weight were 84.8 cm (−5.9 SD) and 10 kg (−3 SD), respectively. He was moderately mentally retarded.

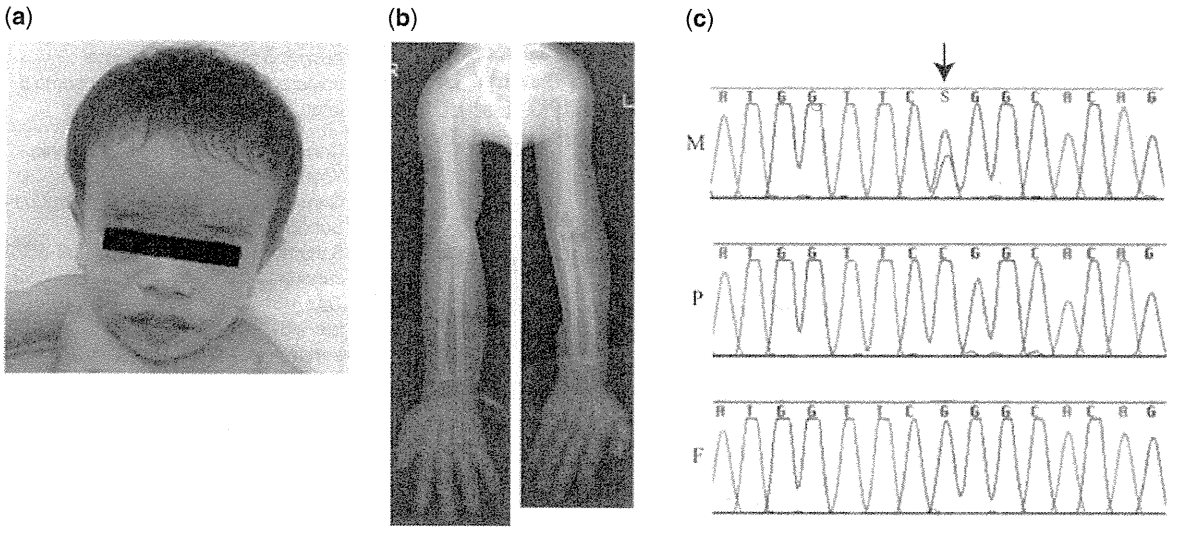

Fig. 1. Facial and skeletal features of the patient at 2 years 7 months of age. (**a**) Note the inverted triangular gloomy face, short nose, full lips, and long philtrum. (**b**) Note the slender long bones. (**c**) Electropherograms of the patient and parents. DNA sequence showing a single base change substituting cytosine for guanine, which results in p.R992P, in the patient. M, mother; P, patient; and F, father.

Conventional cytogenetic studies and FISH analysis

We obtained blood samples under written informed consent for participation in this study. Conventional cytogenetic examination of G-banded chromosomes from peripheral blood lymphocytes was performed. We also performed fluorescence *in situ* hybridization (FISH) analysis on lymphocyte metaphase spreads from the patient using two Bacterial Artificial Chromosome (BAC) clones containing *CUL7*, RP11-628J2 and RP11-653G5, as probes.

Genomic sequencing

Genomic DNA was extracted from peripheral blood following standard protocols. For mutation analysis, we designed primers to amplify all the coding exons of *CUL7* and the flanking intron sequences. Direct sequencing was carried out using a BigDye Terminator v3.1 Cycle sequencing Kit™ and separated on a Genetic Analyzer 3130*xl* (Applied Biosystems Inc., Foster City, CA). Sequence electropherograms were aligned with SEQUENCHER™ software (Gendcodes, Ann Arbor, MI) to visually inspect base alterations.

Microarray analysis

We performed genome-wide single nucleotide polymorphism (SNP) genotyping using Genome-Wide Human SNP Array 6.0 (SNP6.0) following the manufacturer's instructions (Affymetrix, Santa Clara, CA, http://www.affymetrix.com/index.affx). The data generated from Genotyping Console (GTC) 4.0 were loaded into CHROMOSOME ANALYSIS SUITE (CHAS) 1.0.1 software to display the results. We carried out UPD analyses of the patient using genotype data in trio. Genomic positions of SNPs corresponded to the March 2006 human genome (hg18).

Results

Genomic sequencing

We sequenced all 26 coding exons and flanking intronic regions of the *CUL7* gene, which spans a genomic region of approximately 16.3 kb, in the family. In the patient, we detected a homozygous missense mutation (c.2975G>C) in exon 15, which resulted in the substitution of proline for arginine at amino acid residue 992 (p.R992P) (Fig. 1c). The mother was a heterozygous carrier of the mutation, whereas the father was homozygous for the wild-type allele (Fig. 1c). The p.R992P mutation was not detected in 100 unrelated control individuals.

Conventional and molecular cytogenetic analyses

G-banding and FISH analysis at the *CUL7* locus showed a normal karyotype in the patient and the parents with no microdeletion at *CUL7* locus in the patient (data not shown).

Microarray analysis

To confirm paternity, and to find a small size deletion, we performed SNP6.0 analysis. However, no copy number variations (CNVs) were identified in the region containing both *CUL7* and *OBSL1* genes (Fig. 2a). The other variants overlap with reported regions of CNVs in the Database of Genomic Variants (http://projects.tcag.ca/variation) or were transmitted from the parents (data not shown).

To confirm matUPD6 in the patient, we examined the genotypes of the patient/father/mother trio. The results using informative markers indicated that there were two maternal heterodisomic regions (hUPD6-1 and hUPD6-2) and two maternal isodisomic regions (iUDP6-1 and iUPD6-2) in chromosome 6, respectively (Fig. 2 and Table 1). The results indicated that the patient had inherited two alleles from his mother, but none from his father, in chromosome 6. The final karyotype of this patient was 46,XY,upd(6)mat and arr 6p25.3p22.3(110,391–16,287,166)×2 htz mat,6p 22.3q12(16,290,223–65,796,893)×2 hmz mat,6q 12q25.1(65,799,990–150,517,779)×2 htz mat,6q 25.1q27(150,518,012–170,759,956)×2 hmz mat.

Discussion

We identified a causative homozygous mutation in *CUL7* in a patient with 3M syndrome. The results clearly indicate that mat-iUPD6 involving a mutant allele of the *CUL7* gene caused 3M syndrome in the patient.

matUPD6 is relatively rare and seven cases have been reported. The first case was a renal transplant patient who showed growth retardation at birth and mat-iUPD6 (12). The second case was a patient with congenital adrenal hyperplasia (CAH) resulting from a homozygous mutation in the 21-hydroxylase gene (*CYP21*), and had intrauterine growth retardation (IUGR) and mat-iUPD6 (13). The third case was a macerated male fetus from a pregnancy terminated at 23 weeks of gestation because of intrauterine death. The patient showed a mosaic trisomy 6 (14). The fourth case was a male patient with two clinical phenotypes, Klinefelter's syndrome and CAH. His karyotype was mosaic 48,XXY, +mar[30]/47,XXY[20] and

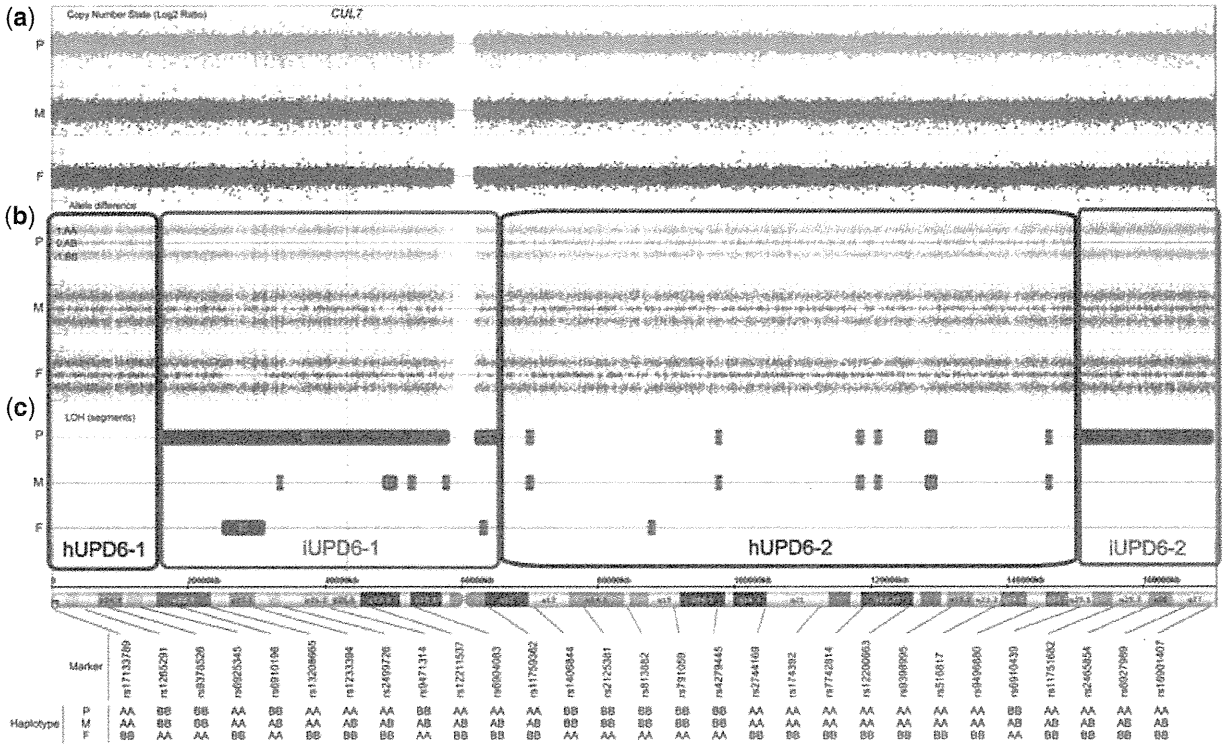

Fig. 2. SNP6.0 data. (**a**) Plots of the SNP6.0 data displayed in ChAS 1.0.1 showing the log2 ratio plot of copy number state, allele difference plot, and loss of heterozygosity (LOH) segment (purple box) (P, patient; M, mother; and F, father). (**b**) The allele difference graph represents the genotypes for each individual single nucleotide polymorphism (SNP). Dots with a value of 1, −1, and 0 represent SNPs with AA, BB, and AB genotypes, respectively. A vertical dashed line indicates the *CUL7* locus. (**c**) The LOH segment plot indicates nine LOH regions on chromosome 6. iUPD6-1 and iUPD6-2 denote the regions of uniparental isodisomy (red box). hUPD6-1 and hUPD6-2 denote the regions of uniparental heterodisomy (blue box). The genotypes on chromosome 6 indicate maternal heterodisomy or isodisomy in the affected offspring [only the uniparental disomy (UPD) markers are displayed].

Table 1. Examination of SNPs from a patient/father/mother trio[a]

			hUPD6-1	iUPD6-1	hUPD6-2	iUPD6-2
Genotype of trio (patient/father/mother)	iUPD	AA/BB/AB	0	534	0	318
		BB/AA/AB	0	576	3	304
	iUPD or hUPD	AA/BB/AA	178	543	605	272
		BB/AA/BB	196	506	563	262
Share genotype (patient/mother)	iUPD or hUPD	AA/AA	2,812	5,897	9,716	3,009
		BB/BB	2,799	5,785	9,557	2,919
	hUPD	AB/AB	1,699	19	6,384	12
		Total of share genotype	7,310	11,701	25,657	5,940
		Share genotype rate (%)	99.82	78.20	99.89	73.31
		Total SNP probe	7,323	14,963	25,684	8,103
		Start SNP	rs4959515	rs9370869	rs9354209	rs9384189
		Start position	110,391	16,290,223	65,799,990	150,518,012
		End SNP	rs9477050	rs9453156	rs7765984	rs6931065
		End position	16,287,166	65,796,893	150,517,779	170,759,956
		Size (bp)	16,176,776	49,506,671	84,717,790	20,241,945
		Cytoband	p25.3-p22.3	p22.3-q12	q12-q25.1	q25.1-q27

hUPD, uniparental heterodisomy; iUPD, uniparental isodisomy; iUPD or hUPD, UPD could not be defined as isodisomy or heterodisomy; SNP, single nucleotide polymorphism.

[a]Each row contains information on each matUPD6 inheritance block identified by trio haplotype analysis.

both the X chromosome and chromosome 6 showed maternal iUPD. This case also was notable for IUGR and growth retardation at 8 months of age (15). The fifth case was a fetus with IUGR at 29 weeks of pregnancy from a 45-year-old patient. The case was ascertained as trisomy 6 mosaicism in cultured chorionic villi but disomy in amniocytes; analysis of DNA markers in amniocytes and parental samples revealed mat-iUPD6 in disomy cells (16). The sixth case was a male infant with molybdenum cofactor deficiency who showed developmental delay. SNP analysis with the trio revealed that at least 6p21.1-6p24.3 were mat-iUPD6, but not another region were remain unclear (17). The seventh case was a patient with cleft lip and palate, and showed a complete maternal hUPD on chromosome 6 (mat-hUPD6). This case had no notable IUGR in the serial ultrasound examination (18). Taken together, IUGR and growth retardation were found in the cases with mat-iUPD6 (12, 13, 15–17), while these were not found in cases with mat-hUPD6 (14, 18). The IUGR and growth retardation in cases of mat-iUPD6 may be the result of homozygosity of chromosome 6. On the basis of these reports, no clear maternal imprinting effect of chromosome 6 can be established; however, recently, a complete gain of methylation phenotype at insulin-like growth factor 2 receptor was shown in patients with growth restriction (19).

The patient with homozygous mutation in *CUL7* and matUPD6 had clinical features compatible with 3M syndrome. However, the patient displayed certain features that have not been previously reported among patients with *CUL7* mutations such as mild mental retardation, inguinal hernia, hydrocele testis, and mild ventricular enlargement (7, 8, 20). Mild mental retardation is an especially characteristic phenotype in our case because most patients with 3M syndrome have normal intelligence. It is difficult to determine whether matUPD6 had a significant role in the development of certain feature in our case.

Here we report a case of 3M syndrome with a homozygous mutation that resulted from maternal iUPD, including the *CUL7* gene. Although complete paternal or maternal UPD for chromosome 6 has previously been reported, this is the first report of a patient with 3M syndrome who has a mixture of mat-hUPD6 and mat-iUPD6 regions. Our results emphasize that UPD should be considered possible mechanism for developing the autosomal recessive disorders including 3M syndrome.

Acknowledgements

We are grateful to the patient and his parents for their participation in this research. We also thank Ms Miho Ooga and Ms Chisa Hayashida for technical assistance. K.-I. Y. was supported in part by Grants-in-Aid for Scientific Research from the Ministry of Health, Labour and Welfare, and in part by the Takeda Scientific Foundation and the Naito Foundation.

References

1. Winter RM, Baraitser M, Grant DB, Preece MA, Hall CM. The 3-M syndrome. J Med Genet 1984: 21: 124–128.
2. Feldmann M, Gilgenkrantz S, Parisot S, Zarini G, Marchal C. 3M dwarfism: a study of two further sibs. J Med Genet 1989: 26 (9): 583–585.
3. García-Cruz D, Cantú JM. Heterozygous expression in 3-M slender-boned nanism. Hum Genet 1979: 52: 221–226.
4. Mueller RF, Buckler J, Arthur R et al. The 3-M syndrome: risk of intracerebral aneurysm? J Med Genet 1992: 29: 425–427.
5. Le Merrer M, Brauner R, Maroteaux P. Dwarfism with gloomy face: a new syndrome with features of 3-M syndrome. J Med Genet 1991: 28: 186–191.
6. Spranger J, Opitz JM, Nourmand A. A new familial intrauterine growth retardation syndrome the "3-M syndrome". Eur J Pediatr 1976: 123: 115–124.
7. Huber C, Dias-Santagata D, Glaser A et al. Identification of mutations in *CUL7* in 3-M syndrome. Nat Genet 2005: 37: 1119–1124.
8. Huber C, Delezoide AL, Guimiot F et al. A large-scale mutation search reveals genetic heterogeneity in 3M syndrome. Eur J Hum Genet 2009: 17: 395–400.
9. Hanson D, Murray PG, Sud A et al. The primordial growth disorder 3-M syndrome connects ubiquitination to the cytoskeletal adaptor *OBSL1*. Am J Hum Genet 2009: 84: 801–806.
10. Huber C, Fradin M, Edouard T et al. OBSL1 mutations in 3-M syndrome are associated with a modulation of IGFBP2 and IGFBP5 expression levels. Hum Mutat 2010: 31: 20–26.
11. Engel E. A new genetic concept: uniparental disomy and its potential effect, isodisomy. Am J Med Genet 1980: 6: 137–143.
12. van den Berg-Loonen EM, Savelkoul P, van Hooff H, van Eede P, Riesewijk A, Geraedts J. Uniparental maternal disomy 6 in a renal transplant patient. Hum Immunol 1996: 45: 46–51.
13. Spiro RP, Christian SL, Ledbetter DH et al. Intrauterine growth retardation associated with maternal uniparental disomy for chromosome 6 unmasked by congenital adrenal hyperplasia. Pediatr Res 1999: 46: 510–513.
14. Cockwell AE, Baker SJ, Connarty M, Moore IE, Crolla JA. Mosaic trisomy 6 and maternal uniparental disomy 6 in a 23-week gestation fetus with atrioventricular septal defect. Am J Med Genet A 2006: 140: 624–627.
15. Parker EA, Hovanes K, Germak J, Porter F, Merke DP. Maternal 21-hydroxylase deficiency and uniparental isodisomy of chromosome 6 and X results in a child with 21-hydroxylase deficiency and Klinefelter syndrome. Am J Med Genet A 2006: 140: 2236–2240.
16. Haag M, Beischel L, Rokeach J et al. First prenatal detection of maternal uniparental disomy (UPD) of chromosome 6 and 'rescue' of trisomy 6 [abstract]. *Abstracts of the 57th Annual Meeting of the ASHG 2007*; Abstract no 2428.
17. Gümüş H, Ghesquiere S, Per H et al. Maternal uniparental isodisomy is responsible for serious molybdenum cofactor deficiency. Dev Med Child Neurol 2010: 52 (9): 868–872.

18. Salahshourifar I, Halim AS, Sulaiman WA, Zilfalil BA. Maternal uniparental heterodisomy of chromosome 6 in a boy with an isolated cleft lip and palate. Am J Med Genet A 2010: 152A (7): 1818–1821.
19. Turner CL, Mackay DM, Callaway JL et al. Methylation analysis of 79 patients with growth restriction reveals novelpatterns of methylation change at imprinted loci. Eur J Hum Genet 2010: 18: 648–655.
20. Maksimova N, Hara K, Miyashia A et al. Clinical, molecular and histopathological features of short stature syndrome with novel *CUL7* mutation in Yakuts: new population isolate in Asia. J Med Genet 2007: 44: 772–778.

CLINICAL REPORT

AMERICAN JOURNAL OF medical genetics PART A

A De Novo Deletion of 20q11.2–q12 in a Boy Presenting With Abnormal Hands and Feet, Retinal Dysplasia, and Intractable Feeding Difficulty

Yoko Hiraki,[1,2] Akira Nishimura,[2] Michiko Hayashidani,[3] Yoshiko Terada,[4] Gen Nishimura,[5] Nobuhiko Okamoto,[6] Sachiko Nishina,[7] Yoshinori Tsurusaki,[2] Hiroshi Doi,[2] Hirotomo Saitsu,[2] Noriko Miyake,[2] and Naomichi Matsumoto[2]*

[1]Hiroshima Municipal Center for Child Health and Development, Hiroshima, Japan

[2]Department of Human Genetics, Yokohama City University Graduate School of Medicine, Yokohama, Japan

[3]Medical Center for Premature and Neonatal Infants, Hiroshima City Hospital, Hiroshima, Japan

[4]Department of Ophthalmology, Hiroshima City Hospital, Hiroshima, Japan

[5]Department of Pediatric Imaging, Tokyo Metropolitan Children's Medical Center, Tokyo, Japan

[6]Department of Medical Genetics, Osaka Medical Center and Research Institute for Maternal and Child Health, Osaka, Japan

[7]Department of Ophthalmology, National Center for Child Health and Development, Tokyo, Japan

Received 18 June 2010; Accepted 23 October 2010

Proximal interstitial deletions involving 20q11–q12 are very rare. Only two cases have been reported. We describe another patient with 20q11.21–q12 deletion. We precisely mapped the 6.5-Mb deletion and successfully determined the deletion landmarks at the nucleotide level. Common clinical features among the three cases include developmental delay, intractable feeding difficulties with gastroesophageal reflux, and facial dysmorphism including triangular face, hypertelorism, and hypoplastic alae nasi, indicating that the 20q11.2–q12 deletion can be a clinically recognizable syndrome. This is also supported by the fact that the three deletions overlap significantly. In addition, unique features such as arthrogryposis/fetal akinesia (hypokinesia) deformation and retinal dysplasia are recognized in the patient reported herein. © 2011 Wiley-Liss, Inc.

Key words: 20q interstitial deletion; abnormal hands and feet; retinal dysplasia; feeding difficulty

How to Cite this Article:
Hiraki Y, Nishimura A, Hayashidani M, Terada Y, Nishimura G, Okamoto N, Nishina S, Tsurusaki Y, Doi H, Saitsu H, Miyake N, Matsumoto N. 2011. A de novo deletion of 20q11.2–q12 in a boy presenting with abnormal hands and feet, retinal dysplasia, and intractable feeding difficulty.
Am J Med Genet Part A.

INTRODUCTION

Interstitial deletions of the long arm of chromosome 20 are rare. To our knowledge, a total of 12 patients have been reported in the literature [Petersen et al., 1987; Shabtai et al., 1993; Aldred et al., 2002; Genevieve et al., 2005; Callier et al., 2006; Borozdin et al., 2007; Iqbal and Al-Owain, 2007]. Among them, only two cases showed the proximal q deletion (20q11–q12), not extending to q13 [Callier et al., 2006; Iqbal and Al-Owain, 2007]. One patient had a 6.6-Mb deletion at 20q11.21–q11.23 [Callier et al., 2006], and the other [Iqbal and Al-Owain, 2007] showed a 6.8-Mb deletion at 20q11.2–q12. Here, we report on the third patient with a 6.5-Mb deletion at 20q11.21–q12, clinically showing mental retardation, minor craniofacial anomalies, and intractable feeding difficulties. The deletion has been precisely analyzed at the nucleotide level and his detailed clinical manifestations will be presented.

Grant sponsor: Japan Society for the Promotion of Science (JSPS); Grant sponsor: Ministry of Health, Labour and Welfare; Grant sponsor: Ministry of Education, Culture, Sports, Science and Technology of Japan; Grant sponsor: Scientific Research.

*Correspondence to:
Naomichi Matsumoto, Department of Human Genetics, Yokohama City University Graduate School of Medicine, Fukuura 3-9, Kanazawa-ku, Yokohama 236-0004, Japan. E-mail: naomat@yokohama-cu.ac.jp

Published online in Wiley Online Library (wileyonlinelibrary.com).
DOI 10.1002/ajmg.a.33818

CLINICAL REPORT

The 18-month-old boy was the first product of healthy 22-year-old mother and 25-year-old father without any consanguinity. Pregnancy was uneventful. Family history was unremarkable. He was born by spontaneous vaginal delivery at 38 weeks of gestation. Birth weight was 2,230 g (−1.7 SD), length 44.0 cm (−1.9 SD), and OFC 32.5 cm (−0.3 SD). Multiple malformations including patent ductus arteriosus, patency of foramen ovale, and dysmorphic face were noted. He was tube-fed due to poor swallowing and oxygen therapy was required until 4 months because of respiratory disturbance. X-ray examination at age of 1 month revealed small thorax and mild slender long bones. In addition, right eye retinal fold was pointed out. At age of 3 months, upper gastrointestinal tract was investigated because of recurrent vomiting, and gastroesophageal reflux (GER) and esophageal hiatus hernia were found. Esophageal hiatus hernia was alleviated spontaneously, but GER persisted.

At age of 4 months, he was referred to us for evaluation of his developmental delay. He was noted to have the following craniofacial features: triangular face, premature closure fontanelle, slopping forehead, wide bending eyebrows, hypertelorism, low-set and posterior rotated ears, long columella nasi, mild hypoplastic alae nasi, short and well-defined philtrum, thin lips with tucked-in lower lip, submucosal cleft palate, microretrognathia and posterior low hair-line (Fig. 1A,B and Table I). Additionally, abnormal hands and feet were recognized, consisted of restriction of all proximal interphalangeal joints and over-extension of all distal interphalangeal joints of hands and feet, radial deviation of 2nd fingers, clinodactyly of the 2nd and 5th fingers, lack of flexion creases bilaterally, right preaxial polydactyly, left single palmar, and talipes valgus. Mild restriction of elbow, hip and knee joints bilaterally was also noted (Fig. 1C–E and Table I).

At 15 months, his weight was 7.5 kg (−2.3 SD), length 71.8 cm (−2.7 SD), and OFC 44.4 cm (−1.6 SD). He could roll over one side and shift a toy from one hand to the other. Social smile was seen, but he could not recognize his parents (DQ 48). His dysphagia persisted based on the modified swallowing study [Kanda et al., 2005]; he required tube-feeding, and rejected oral intake. Ophthalmic examination at 15 months revealed broom-like pattern of retinal vessels extending from optic disc to periphery with a falciform retinal fold in the right eye, causing visual impairment. In the left eye, mild opacity in the lateral portion of vitreous body was found. These findings led to the diagnosis of bilateral retinal dysplasia. Anterior segment and optic disc were normal. Left hearing loss was suspected by auditory brainstem response, otoacoustic emission, and behavioral observation audiometry. Brain magnetic resonance imaging revealed cortical atrophy and mild ventriculomegaly. Blood biochemistry and abdominal ultrasonographic examination were all normal. Serological TORCH (toxoplasma, rubella, cytomegarovirus, and herpes simplex) testing was negative. At 18 months, the shortening of 5th middle phalanges of fingers and absence of middle phalanges of the toes were confirmed by X-ray examination.

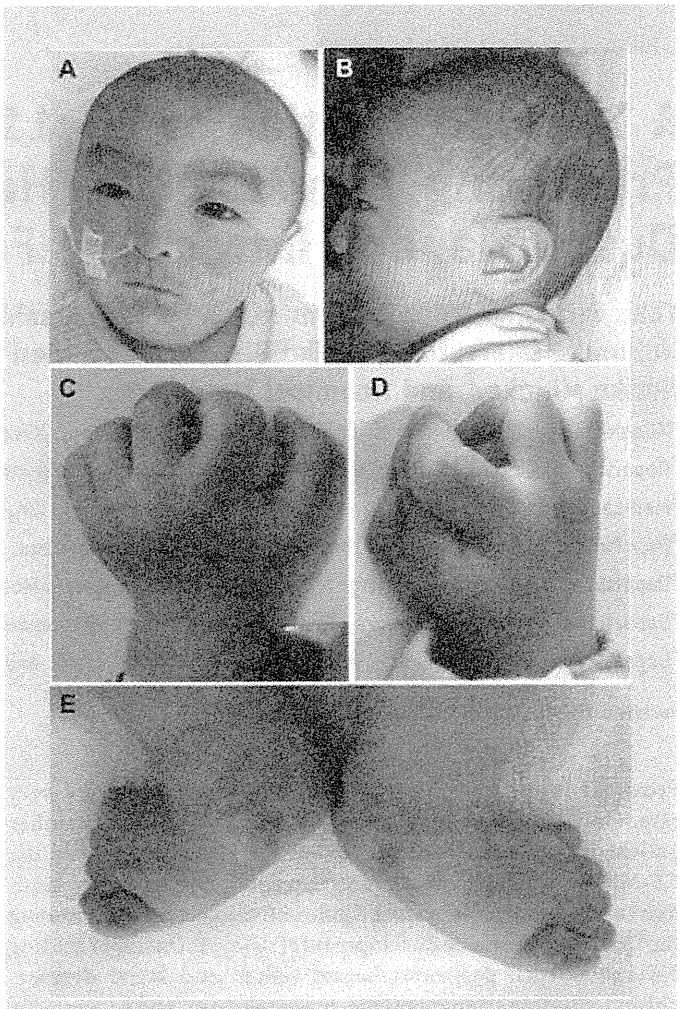

FIG. 1. Photographs of the patient at age of 4 months. A,B: Facial abnormalities including triangular face, wide and bending eyebrows, hypertelorism, long columella, thin lips with tucked-in lower lip, and microretrognathia were recognized. C (left hand) and D (right): Bilateral camptodactyly associated with radial deviation of the 2nd fingers and clinodactyly of the 2nd and 5th, and right preaxial polydactyly were noted. E: Camptodactyly with talipes valgus in both feet.

CYTOGENETIC AND MOLECULAR ANALYSIS

G-banded chromosomal analysis (550 bands level) of the patient's blood lymphocytes indicated normal karyptype (46,XY) (data not shown). Fluorescence in situ hybridization (FISH) analysis using all chromosomal subtelomeric clones did not show any abnormalities. Array CGH analysis using NimbleGen 385K Array (Roche NimbleGen, Inc., Madison, WI) demonstrated a 6.5-Mb heterozygous deletion at 20q11.2–q12 (UCSC genome coordinates 2006 Mar. version, chromosome 20: 31,269,661–37,782,841 bp) (Fig. 2A). The deletion was also confirmed by FISH using BACs (RP11-322B6 and RP11-782C16 at 21q11.21, and RP11-54P22 and RP11-467J15 at 20q12), RP11-787C16 and RP11-54P22 was deleted while RP11-322B6 and RP11-467J15 were not deleted (Fig. 3). The deletion junction was successfully amplified by PCR using primers (Primer A: 5′-TGA TAG AGC CAA CTG GGT CAT GTG C-3′, Primer C: 5′-TCT AGC TTG CTG AAT TCC TGC CTG A-3′) (Fig. 2B) and its product was sequenced. The deleted region was from 31,274,015 to 37,783,826 bp (6,509,811 bp) with 5-bp overlap (ATAGA) (Fig. 2C). The deletion occured de novo as FISH and

TABLE I. Clinical Manifestations of Reported Cases of 20q11–q12 Deletion

	Calliers' case (4 y, female)	Iqbals' case (2 y, male)	Present case (18 m, male)
General			
Growth retardation	+	+	+
Developmental delay	+	+	+
Autistic behavior	+	+	+
Sensory abnormalities/self-injury	+	+	+
Feeding difficulties	+	+	+
Gastroesophageal reflux	+	+	+
Gastrointestinal abnormalities	+ (Pyloric stenosis)	−	+ (Esophageal hiatus hernia)
Feeding intolerance	+ (Diarrhea, vomiting)	−	−
Dysphagia			+
Food refusal	+		+
Muscle tone	Hypertonia	Normal tone except for difficulty in extending the hips	Normal tone
Hearing loss		+	+
Congenital heart defect	−	−	+
Seizure/epilepsy		−	+
Central nervous system			
Cerebral atrophy	+	+	+
Craniofacial			
Triangular face	+	+	+
Hypertelorism	+	+	+
Hypoplastic alae nasi	+	+	+
Sparse hair	+		+
Down-slanting palpebral fissures	+		+
Long columella	+		+
Short, well-defined philtrum	+		+
Thin lips	+		+
Microretrognathia	+		+
Low-set ears	+		+
Extremities			
Arthrogryposis			+
Preaxial polydactyly			+
Clinodactyly of 5th fingers	+		+
Talipes equinovarus		+	
Talopes valgus			+
Ocular			
Retinal dysplasia			+
Microphthalmia		+	−
Duane anomaly		+	n.d.
Strabismus	+		−
Others			
Genital anomlies		+	−

Shadow indicates common features among three cases. y, year(s); m, month(s); +, positive; −, negative; n.d., not determined.

junction PCRs denied the deletion in parental samples (FISH data not shown and Fig. 2B by PCR using primers A, B, and C [primer B: 5′-AGC TGC TCA AAG TGG GGT ATT CTG G-3′]).

DISCUSSION

In this study, we precisely analyzed the 6.5-Mb deletion at 20q11.2–q12 in a boy, presenting with abnormal hands and feet, retinal dysplasia, and intractable feeding difficulty. Proximal interstitial deletions of 20q11–q12 are very rare. Only two cases have been reported and analyzed either by chromosomal CGH and FISH analysis or BAC array CGH with 1-Mb resolution [Callier et al., 2006; Iqbal and Al-Owain, 2007]. Clinical features are presented in Figure 1 and summarized in Table I. Three deletions are overlapping and the shortest region of overlap is from 20q11.22 to q11.23 (Fig. 3). Common clinical features among three cases are

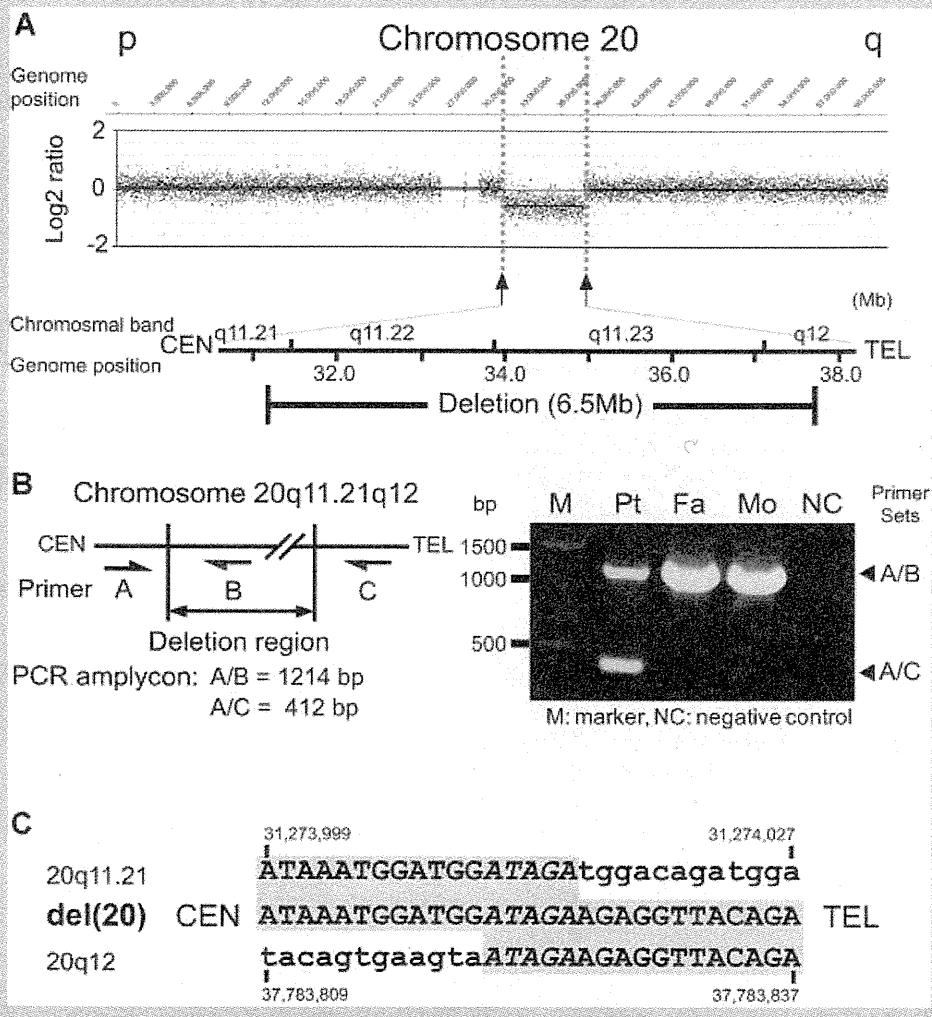

FIG. 2. Analysis of the 20q11.21–q12 deletion. A: High-resolution SNP array revealed the 6.5-Mb deletion at 20q11.21–q12. In the upper part, *Y* and *X* axes indicate probe signal intensity (log 2 ratio) and probe position in chromosome 20, respectively, and in the lower, chromosomal bands together with location of the deletion are shown. B: PCR system (left) to delineate the deletion and its result (right). C: Deletion junction sequence. Upper and lower sequences are normal ones around at proximal [20q11.21] and distal [20q12] deletion breakpoints, respectively. Middle shows the deletion junction in the patient. Gray shadow indicates matched sequences.

growth/developmental retardation, intractable feeding difficulties with GER, cerebral atrophy, and dysmorphic face including triangular face, hypertelorism, and hypoplastic alae nasi. In addition, two out of three patients shared many other facial dysmorphism including sparse hair, downslanting palpebral fissures, long columella, short and well-defined philtrum, thin lips, microretrognathia, and low-set ears. These findings suggest that the 20q11.22–q11.23 deletion can be a recognizable microdeletion syndrome. In addition, unique findings of hands and feet abnormalities as well as retinal dysplasia were found in our patient.

Intractable feeding difficulties in the three patients, is the largest concern for the family, and are speculated to be caused by combined factors: prolonged dysphagia (in our case), aspiration associated with GER (in all three), upper gastrointestinal tract abnormalties (pyloric stenosis [Callier et al., 2006] or esophageal hiatus hernia in our case), vomiting/diarrhea because of feeding intorerance [Callier et al., 2006], sensory abnormalities (in all), and food refusal (in the Callier et al. and our patient).

According to UCSC genome browser (March 2006 assembly), the 6.5-Mb deleted segment identified in our patient encompasses at least 96 known genes, including nine genes related to human disorders. One of these is growth/differentiation factor-5 (*GDF5*, also known as *CDMP1*). This is a protein which belongs to the GDF-subgroup of BMPs and plays an key regulatory role in embryonic skeletal and joint development. *GDF5* abnormalities are known to cause a variety of different skeletal disorders. Interestingly, Everman et al. [2002] and Yang et al. [2008] indicated that functional *GDF5* haploinsufficiency was the culprit of brachydactyly type C (BDC,

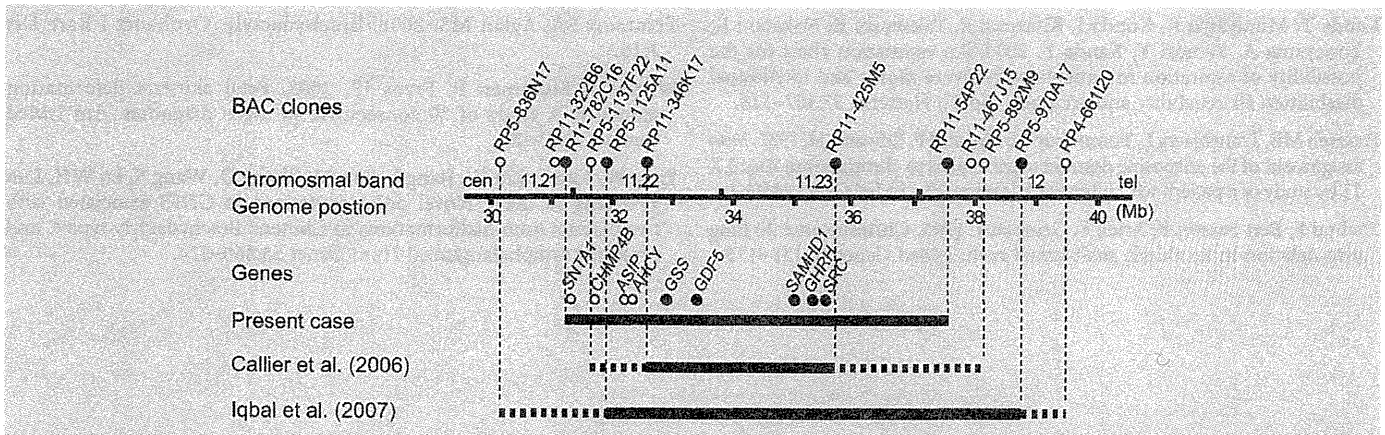

FIG. 3. Shematic presentation of the 20q11–q12 deletions. From top to bottom, BAC clones delineating deletions of all the cases (filled dot: deleted, open dot: not deleted) [Callier et al., 2006; Iqbal and Al-Owain, 2007], chromosomal bands from 20q11.2 to 20q12, genomic position, OMIM genes, and deleted regions of our case and previous ones. Solid and dotted horizontal lines indicate deleted and unconfirmed regions due to the relatively low resolution of the analytical methods.

OMIM #113100) by in vitro studies. As our patient has the *GDF5* haploinsufficiency, he may have the risk for BDC. However, he did not show this manifestation. He did have polydactyly, talipes valgus, and absence of the middle phalanges of the toes, which have been often found in individuals with BDC [Everman et al., 2002; Temtamy and Aglan, 2008]. Our patient did have a fetal akinesia (or hypokinesia) deformation phenotype (FADP). The short neck, hypertelorism, micrognathia, small thorax, postnatal respiratory disturbance, prolonged feeding difficulty, and slender long bone could represent FADP. FADP is a clinically and genetically heterogeneous constellation arising from fetal akinesia or decrease in utero movement due to intrinsic factors including neuropathy, myopathy, and restrictive dermopathy or extrinsic factors that limit fetal movement (e.g., tetragen exposure or fetal crowding) [Witters et al., 2002; Bamshad et al., 2009]. As extrinsic factors (e.g., abnormality of amniotic fluid, fetal crowding, congenital infection, and use of the drug in utero) could not be confirmed in this patient and the arthrogryposis and FADP are accompanied by other organ anomalies and developmental delay, the gene(s) at 20q11.21–q11.23 may be a primary intrinsic cause. Unfortunately, as skeletal malformations in the other two cases having the 20q11.2–q12 deletion were not fully described [Callier et al., 2006; Iqbal and Al-Owain, 2007], it is difficult to discuss the relationship between skeletal features and gene(s) in 20q11.2–q12 deletion.

Retinal dysplasia associated with falciform retinal fold and impaired vision was also noted. Retinal dysplasia is defined as abnormal growth and differentiation of embryonic retina either due to in utero environmental factors such as viral infection, tetragen exposure, retinopathy of prematurity or genetic factors. To our knowledge, this is the first description of retinal dysplasia associated with 20q11.2–q12 deletion.

ACKNOWLEDGMENTS

We are grateful to the patient and his family for their participation and support to this study. Grant-in Aid for Japan Society for the Promotion of Science (JSPS) Fellow (A.N.), Research Grants from the Ministry of Health, Labour and Welfare (N.M.), Grant-in-Aid from the Ministry of Education, Culture, Sports, Science and Technology of Japan (N.M.), and Grant-in-Aid for Scientific Research from JSPS (N.M.).

REFERENCES

Aldred MA, Aftimos S, Hall C, Waters KS, Thakker RV, Trembath RC, Brueton L. 2002. Constitutional deletion of chromosome 20q in two patients affected with albright hereditary osteodystrophy. Am J Med Genet 113:167–172.

Bamshad M, Van Heest AE, Pleasure D. 2009. Arthrogryposis: A review and update. J Bone Joint Surg Am 91:40–46.

Borozdin W, Graham JM Jr, Bohm D, Bamshad MJ, Spranger S, Burke L, Leipoldt M, Kohlhase J. 2007. Multigene deletions on chromosome 20q13.13-q13.2 including SALL4 result in an expanded phenotype of Okihiro syndrome plus developmental delay. Hum Mutat 28:830.

Callier P, Faivre L, Marle N, Thauvin-Robinet C, Sanlaville D, Gosset P, Prieur M, Labenne M, Huet F, Mugneret F. 2006. Major feeding difficulties in the first reported case of interstitial 20q11.22-q12 microdeletion and molecular cytogenetic characterization. Am J Med Genet Part A 140A:1859–1863.

Everman DB, Bartels CF, Yang Y, Yanamandra N, Goodman FR, Mendoza-Londono JR, Savarirayan R, White SM, Graham JM Jr, Gale RP, Svarch E, Newman WG, Kleckers AR, Francomano CA, Govindaiah V, Singh L, Morrison S, Thomas JT, Warman ML. 2002. The mutational spectrum of brachydactyly type C. Am J Med Genet 112:291–296.

Genevieve D, Sanlaville D, Faivre L, Kottler ML, Jambou M, Gosset P, Boustani-Samara D, Pinto G, Ozilou C, Abeguile G, Munnich A, Romana S, Raoul O, Cormier-Daire V, Vekemans M. 2005. Paternal deletion of the GNAS imprinted locus (including Gnasxl) in two girls presenting with severe pre- and post-natal growth retardation and intractable feeding difficulties. Eur J Hum Genet 13:1033–1039.

Iqbal MA, Al-Owain M. 2007. Interstitial del(20)(q11.2q12)—Clinical and molecular cytogenetic characterization. Am J Med Genet Part A 143A:1880–1884.

Kanda T, Murayama K, Kondo I, Kitazumi E, Takahashi K, Nakatani K, Yoneyama A, Yamori Y, Kanda Y. 2005. An estimation chart for the possibility of aspiration in patients with severe motor and intellectual disabilities: Its reliability and accuracy. No To Hattatsu 37:307–316.

Petersen MB, Tranebjaerg L, Tommerup N, Nygaard P, Edwards H. 1987. New assignment of the adenosine deaminase gene locus to chromosome 20q13 X 11 by study of a patient with interstitial deletion 20q. J Med Genet 24:93–96.

Shabtai F, Ben-Sasson E, Arieli S, Grinblat J. 1993. Chromosome 20 long arm deletion in an elderly malformed man. J Med Genet 30:171–173.

Temtamy SA, Aglan MS. 2008. Brachydactyly. Orphanet J Rare Dis 3:15.

Witters I, Moerman P, Fryns JP. 2002. Fetal akinesia deformation sequence: A study of 30 consecutive in utero diagnoses. Am J Med Genet 113:23–28.

Yang W, Cao L, Liu W, Jiang L, Sun M, Zhang D, Wang S, Lo WH, Luo Y, Zhang X. 2008. Novel point mutations in GDF5 associated with two distinct limb malformations in Chinese: Brachydactyly type C and proximal symphalangism. J Hum Genet 53:368–374.

RESEARCH ARTICLE

AMERICAN JOURNAL OF medical genetics PART A

Submicroscopic Deletion in 7q31 Encompassing *CADPS2* and *TSPAN12* in a Child With Autism Spectrum Disorder and PHPV

Nobuhiko Okamoto,[1]* Yoshikazu Hatsukawa,[2] Keiko Shimojima,[3] and Toshiyuki Yamamoto[3]

[1]Department of Medical Genetics, Osaka Medical Center and Research Institute for Maternal and Child Health, Osaka, Japan

[2]Department of Ophthalmology, Osaka Medical Center and Research Institute for Maternal and Child Health, Osaka, Japan

[3]Institute for Integrated Medical Sciences, Tokyo Women's Medical University, Tokyo, Japan

Received 23 August 2010; Accepted 9 March 2011

We performed array comparative genomic hybridization utilizing a whole genome oligonucleotide microarray in a patient with the autism spectrum disorders (ASDs) and persistent hyperplastic primary vitreous (PHPV). Submicroscopic deletions in 7q31 encompassing *CADPS2* (Ca^{2+}-dependent activator protein for secretion 2) and *TSPAN12* (one of the members of the tetraspanin superfamily) were confirmed. The *CADPS2* plays important roles in the release of neurotrophin-3 and brain-derived neurotrophic factor. Mutations in *TSPAN12* are a relatively frequent cause of familial exudative vitreoretinopathy. We speculate that haploinsufficiency of *CADPS2* and *TSPAN12* contributes to ASDs and PHPV, respectively.

Key words: *CADPS2*; *TSPAN12*; autism; PHPV; CGH

How to Cite this Article:
Okamoto N, Hatsukawa Y, Shimojima K, Yamamoto T. 2011. Submicroscopic deletion in 7q31 encompassing *CADPS2* and *TSPAN12* in a child with autism spectrum disorder and PHPV.
Am J Med Genet Part A 155:1568–1573.

INTRODUCTION

Autism spectrum disorders (ASDs OMIM %209850) are complex neurodevelopmental conditions characterized by social communication disabilities, no or delayed language development, and stereotyped and repetitive behaviors. A number of studies have confirmed that genetic factors play an important role in ASDs.

About 10% of ASDs are associated with a Mendelian syndrome (e.g., fragile X syndrome, tuberous sclerosis and Timothy syndrome). Cytogenetic approaches revealed a high frequency of large chromosomal abnormalities (3–7% of patients), including the most frequently observed maternal 15q11-13 duplication (1–3% of patients). Association studies and mutation analysis of candidate genes have implicated the synaptic genes *NLGN3*(Neuroligin3 OMIM*300336), *NLGN4* (OMIM*300427) [Jamain et al., 2003], *SHANK3* (OMIM*606230)[Durand et al., 2007; Moessner et al., 2007], *NRXN1*(Neurexin1 MIM + 600565) [Kim et al., 2008], *SHANK2* (OMIM*603290) [Berkel et al., 2010], and *CNTNAP2* (MIM*604569) [Alarcón et al., 2008; Arking et al., 2008] in ASDs. There is increasing evidence that the *SHANK3-NLGN4-NRNX1* postsynaptic density genes play important roles in the pathogenesis of ASDs.

Recently, on association between de novo copy number variation (CNV) and ASDs was revealed. Sebat et al. [2007] performed comparative genomic hybridization (CGH) on the genomic DNA from ASD patients and unaffected subjects to detect de novo CNV. As a result, they identified CNV in 12 out of 118 (10%) patients with sporadic ASD and confirmed de novo CNV were significantly associated with ASDs. Marshall et al. [2008] performed a genome-wide search for structural abnormalities in 427 unrelated ASD patients using SNP microarray analysis and karyotyping. De novo CNV were found in approximately 7% and approximately 2% of idiopathic families with one ASD child, or two or more ASD siblings, respectively. These authors discovered a CNV at 16p11.2 with an approximate frequency of 1%. Glessner et al. [2009] reported the results from a whole-genome CNV study of many European ASD patients and controls and found several new susceptibility genes encoding neuronal cell-adhesion molecules, including *NLGN1* and *ASTN2*, and genes involved in the ubiquitin pathways, including *UBE3A*, *PARK2*, *RFWD2*, and *FBXO40*. The investigators suggested that two gene networks, neuronal cell-

Grant sponsor: Ministry of Health, Labour and Welfare of Japan.
*Correspondence to:
Nobuhiko Okamoto, Department of Medical Genetics, Osaka Medical Center and Research Institute for Maternal and Child Health, 840 Murodo-cho, Izumi, Osaka 594-1101, Japan. E-mail: okamoto@osaka.email.ne.jp
Published online 27 May 2011 in Wiley Online Library (wileyonlinelibrary.com).
DOI 10.1002/ajmg.a.34028

adhesion and ubiquitin degradation, that are expressed within the central nervous system contribute to the genetic susceptibility of ASDs.

The International Molecular Genetic Study of Autism Consortium [1998] previously identified linkage loci on chromosomes 7 and 2, which were termed AUTS1 and AUTS5, respectively. Further genetic studies have provided evidence for AUTS1 being located on chromosome 7q [The International Molecular Genetic Study of Autism Consortium 2001]. Screening for mutations in six genes mapping to 7q, *CUTL1*, *SRPK2*, *SYPL*, *LAMB1*, *NRCAM*, and *PTPRZ1* in 48 unrelated individuals with autism led to the identification of several new coding variants in the *CUTL1*, *LAMB1*, and *PTPRZ1*genes [Bonora et al., 2005].

The human Ca^{2+}-dependent activator protein for secretion 2 (*CADPS2*: OMIM*609978) is also located on chromosome 7q31, which is within the AUTS1 locus [Cisternas et al., 2003]. It is a member of the CAPS/CADPS protein family that regulates the secretion of dense-core vesicles, which are abundant in the parallel fiber terminals of granule cells in the cerebellum and play important roles in the release of neurotrophin-3 (NT-3) and brain-derived neurotrophic factor (BDNF) [Sadakata et al., 2007a,b,c]. BDNF is indispensable for brain development and function, including the formation of synapses. Cisternas et al. [2003] studied *CADPS2* mutations in 90 unrelated autistic individuals, but identified no disease-specific variants. However, Sadakata et al. [2007a] reported that an aberrant, alternatively spliced *CADPS2* mRNA that lacks exon 3 (*CADPS2* Delta exon3) is detected in some patients with ASD.

Persistent hyperplastic primary vitreous (PHPV) is an ocular malformation caused by the presence of a retrolental fibrovascular membrane and the persistence of the posterior portion of the tunica vasculosa lentis and the hyaloid artery. It is often accompanied by microphthalmos, cataracts, and glaucoma. *NDP* (OMIM *300658, X-linked) and *FZD4* (OMIM *604579, dominant) were found to be mutated in unilateral and bilateral PHPV [Shastry, 2009]. These genes also cause Norrie disease and familial exudative vitreoretinopathy (FEVR), which share some clinical features with PHPV. FEVR is a genetically heterogeneous retinal disorder characterized by abnormal vascularization of the peripheral retina, which is often accompanied by retinal detachment. Mutations in the genes encoding *LRP5* (OMIM *603506, dominant and recessive) also cause FEVR. Junge et al. [2009] showed that *Tetraspanin12* (*Tspan12*) is expressed in the retinal vasculature, and loss of *Tspan12* phenocopies defects are seen in Fzd4, *Lrp5*, and *Norrin* mutant mice. *TSPAN12* is one of the members of the tetraspanin superfamily, characterized by the presence of four transmembrane domains. It constitutes large membrane complexes with other molecules. Nikopoulos et al. [2010] applied next-generation sequencing and found a mutation in *TSPAN12* (MIM*613168). Poulter et al. [2010] described seven mutations that were identified in a cohort of 70 FEVR patients without mutations in three known genes. Mutations in *TSPAN12*, which is at 7q31, are a relatively frequent cause of FEVR.

We performed array comparative genomic hybridization (array-CGH) utilizing a 44K whole genome oligonucleotide microarray in a patient with the ASDs and PHPV. Submicroscopic deletions in 7q31 encompassing *CADPS2* and *TSPAN12* were confirmed. We speculate that haploinsufficiency of *CADPS2* and *TSPAN12* contributes to ASD and PHPV, respectively.

CLINICAL REPORT

The patient, a 3-year-old boy, was born to nonconsanguineous healthy Japanese parents. His family history was unremarkable. He was born at 40 weeks' of gestation, his birth weight was 3,100 g, and his birth length was 50.0 cm. After birth, congenital nystagmus was noted, and he did not pursuit objects. An ophthalmological examination revealed bilateral PHPV. Cataract, glaucoma, and FEVR were not present. His gross motor development was normal, and his verbal development was delayed.

At 3 years of age, he came to our hospital for evaluation because of developmental delay. On examination dysmorphic features included a round face, low-set ears, broad eyebrows, apparent hypertelorism, blepharophimosis, hypoplastic alae nasi, a long philtrum, and a small mouth. His visual acuity was low, but he could perform daily activities with some support. In addition, impairment of social interaction, poor social skills, and strict adherence to routine behaviors were noted. He showed stereotypic movements and hyperactivity in his day care room. He was diagnosed as having an ASD according to the DSM-VI criteria. His DQ was 76 according to standard Japanese method. At 3 years and 8 months of age, his height, weight, and head circumference were 88.6 cm (−2.4 SD), 11.7 kg (−1.8 SD), and 46.8 cm (−2.4 S.D), respectively.

The results of routine laboratory tests were unremarkable. G-banded karyotype analysis revealed the following karyotype: 46,XY,inv(4)(p14;q21). Electroencephalography (EEG) showed occipital epileptic discharges. He was free from epileptic seizures.

Ultrasound evaluation revealed echogenic bands in the posterior segments of both globes. Magnetic resonance brain imaging also showed bilateral fibrous intraocular tissue (Fig. 1). However, no specific findings were found in the CNS including the cerebellum.

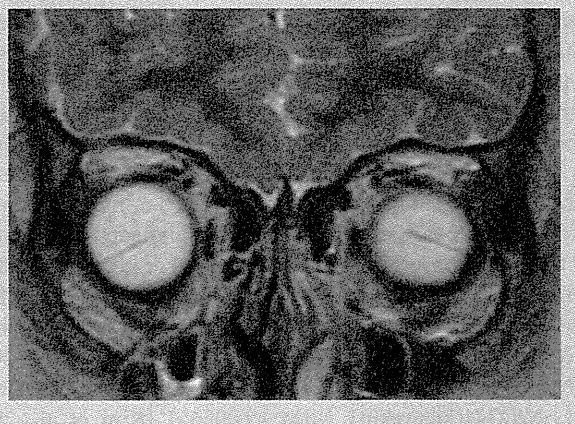

FIG. 1. MR coronal image, T2-weighted. Magnetic resonance imaging also showed fibrous intraocular tissue in the eye. [Color figure can be seen in the online version of this article, available at http://onlinelibrary.wiley.com/journal/10.1002/[ISSN]1552-4833]

MATERIALS AND METHODS

After obtaining informed consent based on a permission approved by the institution's ethical committee, peripheral blood samples were obtained from the patient and his parents. Genomic DNA was extracted using the QIAquick DNA extraction kit (QIAgen, Valencia, CA).

Array-CGH analysis was performed using the Human Genome CGH Microarray 44K (Agilent Technologies, Santa Clara, CA), as described previously [Shimojima et al., 2009].

Metaphase nuclei were prepared from peripheral blood lymphocytes using standard methods and were used for FISH analysis with human BAC clones selected from the UCSC genome browser (http://www.genome.ucsc.edu), as described elsewhere [Shimojima et al., 2009]. Physical positions refer to the March 2006 human reference sequence (NCBI Build 36.1).

RESULTS

Using array-CGH analysis, genomic copy number loss was identified in the 7q31.31 region (Fig. 2). The deletion was 5.4 Mb in size and included *CADPS2* and *TSPAN12*, but not *FOXP2*. There were no copy number changes in chromosome 4. FISH analyses confirmed the above deletion (Fig. 3). There were no deletions in either parent indicating de novo occurrence.

DISCUSSION

We described a patient with an ASD and PHPV who demonstrated submicroscopic deletion in chromosome 7q31.31. The deletion resides in the AUTS1 locus on chromosome 7q. The deleted region contained about 20 genes including *CADPS2* and *TSPAN12*. Little data are available about the association of other genes with developmental and ophthalmological disorders. We posit that haploinsufficiency of *CADPS2* and *TSPAN12* contributes to ASDs and PHPV, respectively.

Our patient fulfilled the DSM-VI criteria for an ASD. Poor eye contact, impairment of social interaction, poor social skills with strict adherence to routine, stereotypic movements, and hyperactivity were noted. However, his intellectual disability was mild. Ataxic movement was not observed.

There have been several reports of small deletions on chromosome 7q. Lennon et al. [2007] reported a young male with moderate intellectual disability, dysmorphic features, and language delay who had a deletion in the 7q31.1-7q31.31 region, which included the *FOXP2* gene. The patient demonstrated language impairment, including developmental verbal dyspraxia, but did not meet the criteria for autism. Cukier et al. [2009] reported a chromosomal inversion spanning the region from approximately 7q22.1 to 7q31 in autistic siblings. They suggested that an autism susceptibility gene is located in the chromosome 7q22–31 region. Dauwerse et al.

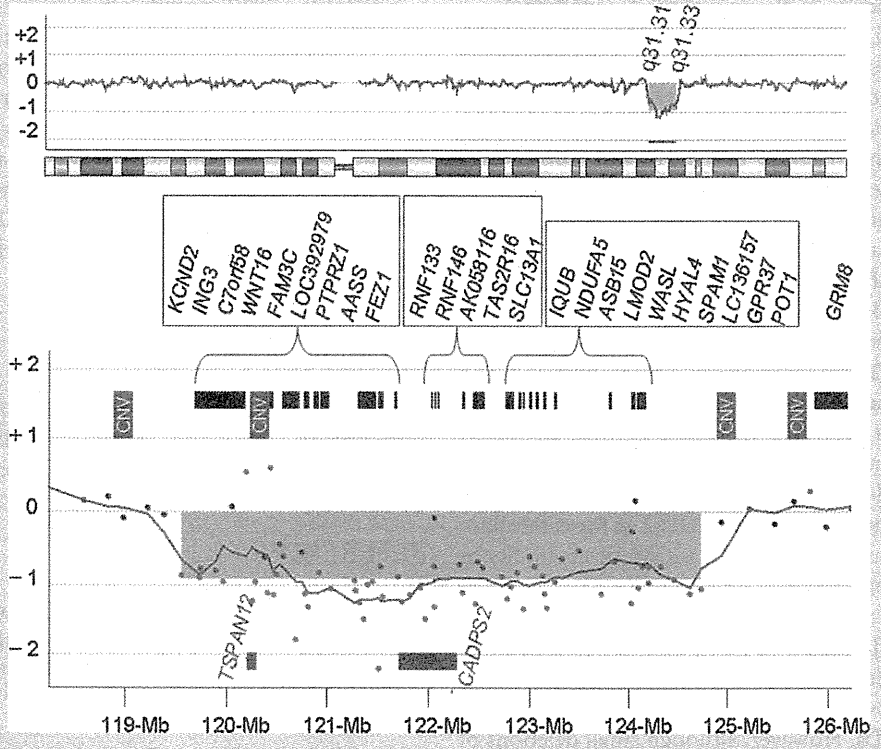

FIG. 2. Array-CGH of the patient. Loss of the genomic copy numbers was identified in the region of 7q31.31. The deletion size was 5.4 Mb and included *CADPS2* and *TSPAN12*.

FIG. 3. FISH analyses of the patient. Arrow head indicates the deletion at 7q31.31.

[2010] characterized a de novo complex rearrangement of the long arm of chromosome 7 in a female patient with moderate mental retardation, anxiety disorder, and autistic features and suggested that disruption of the *C7orf58* gene contributed to the anxiety disorder, and autistic features of their patient. The *C7orf58* gene was also deleted in our patient. However, there have been no basic studies on the association of the *C7orf58* gene and brain function. Further studies are necessary on the role of the *C7orf58* gene.

Sadakata et al. [2007b] studied the behavior of *Cadps2−/−* mice. They showed impaired social interaction, hyperactivity, decreased exploratory behavior, and/or increased anxiety in a novel environment and deficits in intrinsic sleep–wake regulation and circadian rhythmicity. In addition, maternal neglect of newborns was a striking feature. They identified that *Cadps2−/−* mice show deficient release of NT-3 and BDNF. Cerebellar development was impaired in the mice. Sadakata et al. [2007a] found an aberrant alternatively spliced *CADPS2* mRNA that lacks exon 3 in some autistic patients. Exon 3 was shown to encode the dynactin 1-binding domain and affect axonal CADPS2 protein distribution. Exon 3-skipped CADPS2 protein possesses almost normal BDNF releasing activity but is not properly transported into the axons of neocortical or cerebellar neurons. However, Eran et al. [2009] observed no difference in prevalence of exon 3 skipping between ASDs and control samples. They concluded that exon 3 skipping represents a normal, minor isoform of CADPS2 in the cerebellum and is likely not a mechanism underlying autism susceptibility or pathogenesis. Our result may reinforce the evidence that *CADPS2* is associated with ASDs.

Cisternas et al. [2003] studied *CADPS2* gene mutations in 90 unrelated autistic individuals. However, they identified no disease-specific variants. Their results indicate that *CADPS2* mutations are not a major cause of ASDs. However, although small deletions of *CADPS2* as found in the present patient, might be rare, they support the idea that *CADPS2* abnormalities are associated with autism susceptibility.

Nikopoulos et al. [2010] reported two missense mutations in five of 11 FEVR families, indicating that mutations in *TSPAN12* are a relatively frequent cause of FEVR. Both residues are completely conserved throughout vertebrate evolution. These authors suggested that both haploinsufficiency and a dominant-negative effect of the mutant TSPAN12 on the wild-type protein should be considered as underlying disease mechanisms. Poulter et al. [2010] described mutations in the *TSPAN12* gene in FEVR patients and suggested that haploinsufficiency of *TSPAN12* causes FEVR because at least four of the seven mutations are predicted to lead to transcripts with premature-termination codons that are likely to be targeted by nonsense-mediated decay.

Recently, the Norrin/Frizzled4 signaling pathway that acts on the on the surface of developing endothelial cells and controls retinal vascular development is highlighted [Ye et al., 2010]. This pathway is composed of Norrin, its transmembrane receptor, Frizzled4, coreceptor, Lrp5, and an auxiliary membrane protein, Tspan12. The resulting signal controls a transcriptional program that regulates endothelial growth and maturation. PHPV and FEVR are associated with their pathogenesis. Our findings indicate that haploinsufficiency of *TSPAN12* is a plausible causative mechanism for PHPV. It will be interesting to study *TSPAN12* abnormalities in PHPV without *NDP* and *FZD4* mutations.

Singh et al. [2006] reported a voltage-gated potassium channel gene mutation in a temporal lobe epilepsy patient, namely a Kv4.2 truncation mutation lacking the last 44 amino acids in the carboxyl terminal. Kv4.2 channel is encoded by the *KCND2* gene. We suggest that the epileptic discharges on EEG reflect neuronal excitability caused by haploinsufficiency of *KCND2*.

Shen et al. [2010] suggested that using chromosomal microarray analysis to test for submicroscopic genomic deletions and duplications should be considered as part of the initial diagnostic evaluation of patients with ASDs. Miller et al. [2010] suggested that the use of chromosomal microarray is recommended as the first-tier cytogenetic diagnostic test for patients with unexplained developmental delay/intellectual disability, ASDs, or multiple congenital anomalies. In patients with ASDs and other anomalies, chromosomal microarray may be the useful method to clarify the underlying defect.

ACKNOWLEDGMENTS

We thank the patient's family for their cooperation. This study was supported by Health and Labour Research Grants from the Ministry of Health, Labour and Welfare of Japan.

REFERENCES

Alarcón M, Abrahams BS, Stone JL, Duvall JA, Perederiy JV, Bomar JM, Sebat J, Wigler M, Martin CL, Ledbetter DH, Nelson SF, Cantor RM, Geschwind DH. 2008. Linkage, association, and gene-expression analyses identify CNTNAP2 as an autism-susceptibility gene. Am J Hum Genet 82:150–159.

Arking DE, Cutler DJ, Brune CW, Teslovich TM, West K, Ikeda M, Rea A, Guy M, Lin S, Cook EH, Chakravarti A. 2008. A common genetic variant in the neurexin superfamily member CNTNAP2 increases familial risk of autism. Am J Hum Genet 82:160–164.

Berkel S, Marshall CR, Weiss B, Howe J, Roeth R, Moog U, Endris V, Roberts W, Szatmari P, Pinto D, Bonin M, Riess A, Engels H, Sprengel R, Scherer SW, Rappold GA. 2010. Mutations in the SHANK2 synaptic scaffolding gene in autism spectrum disorder and mental retardation. Nat Genet 42:489–491.

Bonora E, Lamb JA, Barnby G, Sykes N, Moberly T, Beyer KS, Klauck SM, Poustka F, Bacchelli E, Blasi F, Maestrini E, Battaglia A, Haracopos D, Pedersen L, Isager T, Eriksen G, Viskum B, Sorensen EU, Brondum-Nielsen K, Cotterill R, Engeland H, Jonge M, Kemner C, Steggehuis K, Scherpenisse M, Rutter M, Bolton PF, Parr JR, Poustka A, Bailey AJ, Monaco AP, International Molecular Genetic Study of Austism Consortium. 2005. Mutation screening and association analysis of six candidate genes for autism on chromosome 7q. Eur J Hum Genet 13:198–207.

Cisternas FA, Vincent JB, Scherer SW, Ray PN. 2003. Cloning and characterization of human CADPS and CADPS2, new members of the Ca^{2+}-dependent activator for secretion protein family. Genomics 81: 279–291.

Cukier HN, Skaar DA, Rayner-Evans MY, Konidari I, Whitehead PL, Jaworski JM, Cuccaro ML, Pericak-Vance MA, Gilbert JR. 2009. Identification of chromosome 7 inversion breakpoints in an autistic family narrows candidate region for autism susceptibility. Autism Res 2: 258–266.

Dauwerse JG, Ruivenkamp CA, Hansson K, Marijnissen GM, Peters DJ, Breuning MH, Hilhorst-Hofstee Y. 2010. A complex chromosome 7q rearrangement identified in a patient with mental retardation, anxiety disorder, and autistic features. Am J Med Genet Part A 152A:427–433.

Durand CM, Betancur C, Boeckers TM, Bockmann J, Chaste P, Fauchereau F, Nygren G, Rastam M, Gillberg IC, Anckarsäter H, Sponheim E, Goubran-Botros H, Delorme R, Chabane N, Mouren-Simeoni MC, de Mas P, Bieth E, Rogé B, Héron D, Burglen L, Gillberg C, Leboyer M, Bourgeron T. 2007. Mutations in the gene encoding the synaptic scaffolding protein SHANK3 are associated with autism spectrum disorders. Nat Genet 39:25–27.

Eran A, Graham KR, Vatalaro K, McCarthy J, Collins C, Peters H, Brewster SJ, Hanson E, Hundley R, Rappaport L, Holm IA, Kohane IS, Kunkel LM. 2009. Comment on "Autistic-like phenotypes in Cadps2-knockout mice and aberrant CADPS2 splicing in autistic patients". J Clin Invest 119: 679–680.

Glessner JT, Wang K, Cai G, Korvatska O, Kim CE, Wood S, Zhang H, Estes A, Brune CW, Bradfield JP, Imielinski M, Frackelton EC, Reichert J, Crawford EL, Munson J, Sleiman PM, Chiavacci R, Annaiah K, Thomas K, Hou C, Glaberson W, Flory J, Otieno F, Garris M, Soorya L, Klei L, Piven J, Meyer KJ, Anagnostou E, Sakurai T, Game RM, Rudd DS, Zurawiecki D, McDougle CJ, Davis LK, Miller J, Posey DJ, Michaels S, Kolevzon A, Silverman JM, Bernier R, Levy SE, Schultz RT, Dawson G, Owley T, McMahon WM, Wassink TH, Sweeney JA, Nurnberger JI, Coon H, Sutcliffe JS, Minshew NJ, Grant SF, Bucan M, Cook EH, Buxbaum JD, Devlin B, Schellenberg GD, Hakonarson H. 2009. Autism genome-wide copy number variation reveals ubiquitin and neuronal genes. Nature 459:569–573.

International Molecular Genetic Study of Autism Consortium. 1998. A full genome screen for autism with evidence for linkage to a region on chromosome 7q. Hum Mol Genet 7:571–578.

International Molecular Genetic Study of Autism Consortium (IMGSAC). 2001. Further characterization of the autism susceptibility locus AUTS1 on chromosome 7q. Hum Mol Genet 10:973–982.

Jamain S, Quach H, Betancur C, Råstam M, Colineaux C, Gillberg IC, Soderstrom H, Giros B, Leboyer M, Gillberg C, Bourgeron T. Paris Autism Research International Sibpair Study. 2003. Mutations of the X-linked genes encoding neuroligins NLGN3 and NLGN4 are associated with autism. Nat Genet 34:27–29.

Junge HJ, Yang S, Burton JB, Paes K, Shu X, French DM, Costa M, Rice DS, Ye W. 2009. TSPAN12 regulates retinal vascular development by promoting Norrin- but not Wnt-induced FZD4/beta-catenin signaling. Cell 139:299–311.

Kim HG, Kishikawa S, Higgins AW, Seong IS, Donovan DJ, Shen Y, Lally E, Weiss LA, Najm J, Kutsche K, Descartes M, Holt L, Braddock S, Troxell R, Kaplan L, Volkmar F, Klin A, Tsatsanis K, Harris DJ, Noens I, Pauls DL, Daly MJ, MacDonald ME, Morton CC, Quade BJ, Gusella JF. 2008. Disruption of neurexin 1 associated with autism spectrum disorder. Am J Hum Genet 82:199–207.

Lennon PA, Cooper ML, Peiffer DA, Gunderson KL, Patel A, Peters S, Cheung SW, Bacino CA. 2007. Deletion of 7q31.1 supports involvement of FOXP2 in language impairment: Clinical report and review. Am J Med Genet A 143A:791–798.

Marshall CR, Noor A, Vincent JB, Lionel AC, Feuk L, Skaug J, Shago M, Moessner R, Pinto D, Ren Y, Thiruvahindrapduram B, Fiebig A, Schreiber S, Friedman J, Ketelaars CE, Vos YJ, Ficicioglu C, Kirkpatrick S, Nicolson R, Sloman L, Summers A, Gibbons CA, Teebi A, Chitayat D, Weksberg R, Thompson A, Vardy C, Crosbie V, Luscombe S, Baatjes R, Zwaigenbaum L, Roberts W, Fernandez B, Szatmari P, Scherer SW. 2008. Structural variation of chromosomes in autism spectrum disorder. Am J Hum Genet 82:477–488.

Miller DT, Adam MP, Aradhya S, Biesecker LG, Brothman AR, Carter NP, Church DM, Crolla JA, Eichler EE, Epstein CJ, Faucett WA, Feuk L, Friedman JM, Hamosh A, Jackson L, Kaminsky EB, Kok K, Krantz ID, Kuhn RM, Lee C, Ostell JM, Rosenberg C, Scherer SW, Spinner NB, Stavropoulos DJ, Tepperberg JH, Thorland EC, Vermeesch JR, Waggoner DJ, Watson MS, Martin CL, Ledbetter DH. 2010. Consensus statement: Chromosomal microarray is a first-tier clinical diagnostic test for individuals with developmental disabilities or congenital anomalies. Am J Hum Genet 86:749–764.

Moessner R, Marshall CR, Sutcliffe JS, Skaug J, Pinto D, Vincent J, Zwaigenbaum L, Fernandez B, Roberts W, Szatmari P, Scherer SW. 2007. Contribution of SHANK3 mutations to autism spectrum disorder. Am J Hum Genet 81:1289–1297.

Nikopoulos K, Gilissen C, Hoischen A, van Nouhuys CE, Boonstra FN, Blokland EA, Arts P, Wieskamp N, Strom TM, Ayuso C, Tilanus MA, Bouwhuis S, Mukhopadhyay A, Scheffer H, Hoefsloot LH, Veltman JA, Cremers FP, Collin RW. 2010. Next-generation sequencing of a 40 Mb linkage interval reveals TSPAN12 mutations in patients with familial exudative vitreoretinopathy. Am J Hum Genet 86:240–247.

Poulter JA, Ali M, Gilmour DF, Rice A, Kondo H, Hayashi K, Mackey DA, Kearns LS, Ruddle JB, Craig JE, Pierce EA, Downey LM, Mohamed MD, Markham AF, Inglehearn CF, Toomes C. 2010. Mutations in TSPAN12 cause autosomal-dominant familial exudative vitreoretinopathy. Am J Hum Genet 86:248–253.

Sadakata T, Washida M, Iwayama Y, Shoji S, Sato Y, Ohkura T, Katoh-Semba R, Nakajima M, Sekine Y, Tanaka M, Nakamura K, Iwata Y, Tsuchiya KJ, Mori N, Detera-Wadleigh SD, Ichikawa H, Itohara S, Yoshikawa T, Furuichi T. 2007a. Autistic-like phenotypes in Cadps2-knockout mice and aberrant CADPS2 splicing in autistic patients. J Clin Invest 117:931–943.

Sadakata T, Kakegawa W, Mizoguchi A, Washida M, Katoh-Semba R, Shutoh F, Okamoto T, Nakashima H, Kimura K, Tanaka M, Sekine Y, Itohara S, Yuzaki M, Nagao S, Furuichi T. 2007b. Impaired cerebellar development and function in mice lacking CAPS2, a protein involved in neurotrophin release. J Neurosci 27:2472–2482.

Sadakata T, Washida M, Furuichi T. 2007c. Alternative splicing variations in mouse CAP S2: Differential expression and functional properties of splicing variants. BMC Neurosci 8:25.

Sebat J, Lakshmi B, Malhotra D, Troge J, Lese-Martin C, Walsh T, Yamrom B, Yoon S, Krasnitz A, Kendall J, Leotta A, Pai D, Zhang R, Lee YH, Hicks

J, Spence SJ, Lee AT, Puura K, Lehtimäki T, Ledbetter D, Gregersen PK, Bregman J, Sutcliffe JS, Jobanputra V, Chung W, Warburton D, King MC, Skuse D, Geschwind DH, Gilliam TC, Ye K, Wigler M. 2007. Strong association of de novo copy number mutations with autism. Science 316:445–449.

Shastry BS. 2009. Persistent hyperplastic primary vitreous: Congenital malformation of the eye. Clin Experiment Ophthalmol 37:884–890.

Shen Y, Dies KA, Holm IA, Bridgemohan C, Sobeih MM, Caronna EB, Miller KJ, Frazier JA, Silverstein I, Picker J, Weissman L, Raffalli P, Jeste S, Demmer LA, Peters HK, Brewster SJ, Kowalczyk SJ, Rosen-Sheidley B, McGowan C, Duda AW III, Lincoln SA, Lowe KR, Schonwald A, Robbins M, Hisama F, Wolff R, Becker R, Nasir R, Urion DK, Milunsky JM, Rappaport L, Gusella JF, Walsh CA, Wu BL, Miller DT. Autism Consortium Clinical Genetics/DNA Diagnostics Collaboration. 2010. Clinical genetic testing for patients with autism spectrum disorders. Pediatrics 125:e727–e735.

Shimojima K, Páez MT, Kurosawa K, Yamamoto T. 2009. Proximal interstitial 1p36 deletion syndrome: The most proximal 3.5-Mb microdeletion identified on a dysmorphic and mentally retarded patient with inv(3)(p14.1q26.2). Brain Development 31:629–633.

Singh B, Ogiwara I, Kaneda M, Tokonami N, Mazaki E, Baba K, Matsuda K, Inoue Y, Yamakawa K. 2006. A Kv4.2 truncation mutation in a patient with temporal lobe epilepsy. Neurobiol Dis 24:245–253.

Ye X, Wang Y, Nathans J. 2010. The Norrin/Frizzled4 signaling pathway in retinal vascular development and disease. Trends Mol Med 16:417–425.

RESEARCH ARTICLE

AMERICAN JOURNAL OF medical genetics PART A

Delineation of Dermatan 4-*O*-sulfotransferase 1 Deficient Ehlers–Danlos Syndrome: Observation of Two Additional Patients and Comprehensive Review of 20 Reported Patients

Kenji Shimizu,[1] Nobuhiko Okamoto,[2] Noriko Miyake,[3] Katsuaki Taira,[4] Yumiko Sato,[5] Keiko Matsuda,[2] Noriko Akimaru,[2] Hirofumi Ohashi,[1] Keiko Wakui,[6] Yoshimitsu Fukushima,[6] Naomichi Matsumoto,[3] and Tomoki Kosho[6]*

[1]Division of Medical Genetics, Saitama Children's Medical Center, Saitama, Japan

[2]Department of Medical Genetics, Osaka Medical Center and Research Institute for Maternal and Child Health, Osaka, Japan

[3]Department of Human Genetics, Yokohama City University Graduate School of Medicine, Yokohama, Japan

[4]Department of Orthopedics, Saitama Children's Medical Center, Saitama, Japan

[5]Department of Radiology, Saitama Children's Medical Center, Saitama, Japan

[6]Department of Medical Genetics, Shinshu University School of Medicine, Matsumoto, Japan

Received 20 January 2011; Accepted 21 April 2011

Loss-of-function mutations in *CHST14*, dermatan 4-*O*-sulfotransferase 1 (D4ST1) deficiency, have recently been found to cause adducted thumb-clubfoot syndrome (ATCS; OMIM-#601776) and a new type of Ehlers–Danlos syndrome (EDS) coined as EDS Kosho Type (EDSKT) [Miyake et al., 2010], as well as a subset of kyphoscoliosis type EDS without lysyl hydroxylase deficiency (EDS VIB) coined as musculocontractural EDS (MCEDS) [Malfait et al., 2010]. Lack of detailed clinical information from later childhood to adulthood in ATCS and lack of detailed clinical information from birth to early childhood in EDSKT and MCEDS have made it difficult to determine whether these disorders would be distinct clinical entities or a single clinical entity with variable expressions and with different presentations depending on the patients' ages at diagnosis. We present detailed clinical findings and courses of two additional unrelated patients, aged 2 years and 6 years, with EDSKT with a comprehensive review of 20 reported patients with D4ST1 deficiency, which supports the notion that these disorders constitute a clinically recognizable form of EDS. The disorder, preferably termed D4ST1-deficient EDS, is characterized by progressive multisystem fragility-related manifestations (joint dislocations and deformities, skin hyperextensibility, bruisability, and fragility; recurrent large subcutaneous hematomas, and other cardiac valvular, respiratory, gastrointestinal, and ophthalmological complications) resulting from impaired assembly of collagen fibrils, as well as various malformations (distinct craniofacial features, multiple congenital contractures, and congenital defects in cardiovascular, gastrointestinal, renal, ocular, and central nervous systems) resulting from inborn errors of development.

How to Cite this Article:
Shimizu K, Okamoto N, Miyake N, Taira K, Sato Y, Matsuda K, Akimaru N, Ohashi H, Wakui K, Fukushima Y, Matsumoto N, Kosho T. 2011. Delineation of Dermatan 4-*O*-sulfotransferase 1 Deficient Ehlers–Danlos Syndrome: Observation of Two Additional Patients and Comprehensive Review of 20 Reported Patients.
Am J Med Genet Part A.

Key words: dermatan 4-*O*-sulfotransferase 1 deficiency; adducted thumb-clubfoot syndrome; Ehlers–Danlos syndrome Kosho type; musculocontractural Ehlers–Danlos syndrome; congenital contractures; progressive multisystem fragility-related manifestations; malformations

Additional supporting information may be found in the online version of this article.

Grant sponsor: Research on Intractable Diseases, Ministry of Health, Labor and Welfare, Japan; Grant number: 2141039040.

Kenji Shimizu, Nobuhiko Okamoto, and Tomoki Kosho have equally contributed to this work.

*Correspondence to:
Tomoki Kosho, MD, Department of Medical Genetics, Shinshu University School of Medicine, 3-1-1 Asahi, Matsumoto 390-8621, Japan.
E-mail: ktomoki@shinshu-u.ac.jp

Published online 00 Month 2011 in Wiley Online Library (wileyonlinelibrary.com).
DOI 10.1002/ajmg.a.34115

INTRODUCTION

Dermatan 4-*O*-sulfotransferase 1 (D4ST1) is a regulatory enzyme in the glycosaminoglycan biosynthesis that transfers active sulfate to position 4 of the *N*-acetyl-D-galactosamine residues of dermatan sulfate [Evers et al., 2001; Mikami et al., 2003]. Dermatan sulfate, as well as chondroitin sulfate and heparan sulfate, constitutes glycosaminoglycan sidechains of proteoglycans; and has been implicated in cardiovascular disease, tumorigenesis, infection, wound repair, and fibrosis via dermatan sulfate-containing proteoglycans such as decorin and biglycan [Trowbridge and Gallo, 2002]. Carbohydrate sulfotransferase 14 (*CHST14*), localized on 15q12, is the gene encoding D4ST1. Recently, loss-of-function mutations in *CHST14* (D4ST1 deficiency) have been found to cause adducted thumb-clubfoot syndrome (ATCS; OMIM#601776) in 11 patients from four families [Dündar et al., 2009] and a variant of Ehlers–Danlos syndrome (EDS) in six patients from six families [Miyake et al., 2010], tentatively coined as EDS Kosho Type (EDSKT) in the London Dysmorphology Database (http://www.lmdatabases.com/index.html) and POSSUM (http://www.possum.net.au/). ATCS was originally recognized as a new type of arthrogryposis, focused on characteristic clinical pictures from birth to early childhood, including adducted thumbs and talipes equinovarus as well as facial dysmorphisms (prominent forehead, large fontanelle, hypertelorism, down-slanting palpebral fissures, low-set ears), and arachnodactyly [Dündar et al., 1997; Sonoda and Kouno, 2000; Dündar et al., 2001; Janecke et al., 2001]. In a recent study by Dündar et al. [2009], ATCS has been categorized again as a connective tissue disorder, based on additional clinical pictures from childhood to adolescence, including skin fragility and bruisability, joint laxity, and osteopenia. EDSKT comprises a pattern of distinct craniofacial features, multiple congenital contractures, progressive joint and skin laxity, and progressive multisystem fragility-related manifestations, including recurrent large subcutaneous hematomas and other cardiac, respiratory, gastrointestinal, ophthalmological complications [Yasui et al., 2003; Kosho et al., 2005, 2010].

Very recently, Malfait et al. [2010] have independently found mutations in *CHST14* in three patients from two families, who were diagnosed with kyphoscoliosis type EDS without lysyl hydroxylase deficiency (EDS VIB). They concluded that their series and ATCS, as well as EDSKT, formed a phenotypic continuum based on their clinical observations and identification of an identical mutation in both conditions, and proposed to coin the disorder as "musculocontractural EDS" (MCEDS) [Malfait et al., 2010]. However, it is still an unsolved problem whether ATCS, EDSKT, and MCEDS would be distinct clinical entities or a single clinical entity with variable inter- and intrafamilial expressions and with different presentations depending on the patients' ages at diagnosis [Miyake et al., 2010], because detailed clinical information are lacking in ATCS from later childhood to adulthood and in EDSKT and MCEDS from birth to early childhood.

Here, we present detailed clinical findings and courses of two additional unrelated patients, aged 2 years and 6 years, with EDSKT, which would contribute to delineate comprehensive phenotypic spectrum of D4ST1 deficiency.

CLINICAL REPORTS

Patient 1

The patient, a Japanese boy, was the second child of a healthy 31-year-old mother and a healthy 33-year-old nonconsanguineous father. He was born by cesarean for breech presentation at 38 weeks and 3 days of gestation. His birth weight was 3,092 g (+0.2 SD), length 46 cm (−1.3 SD), and OFC 34 cm (+0.4 SD). At age 15 days, he was referred to our hospital for the treatment of bilateral talipes equinovarus. He had a round face with a large fontanelle, hypertelorism, short palpebral fissures, blue sclerae, strabismus, a short nose with a hypoplastic columella, low-set and rotated ears, a high palate, a long philtrum, a thin upper lip vermillion, a small mouth, and microretrognathia (Fig. 1A, B). He had arachnodactyly, flexion-adduction contractures of bilateral thumbs, flexion contractures of the interphalangeal (IP) joints in the other fingers, flexion contractures of bilateral elbows and knees, and rigidity of bilateral hip joints (Fig. 1C). He also had widely spaced nipples, a redundant and translucent skin, an umbilical hernia, and bilateral cryptorchidism (Fig. 1C). Talipes equinovarus was treated with incision of bilateral Achilles' tendons at age 2 months, followed by serial plaster casts and braces. Skin fragility was observed at the procedure. It was surgically corrected at age 1 year and 11 months. Gross motor development was delayed: He raised his head at 6 months, sat without support at age 1 year, stood up assisted at age 1 year and 6 months, and walked assisted after surgical correction of talipes equinovarus. He had bruises easily on the occiput

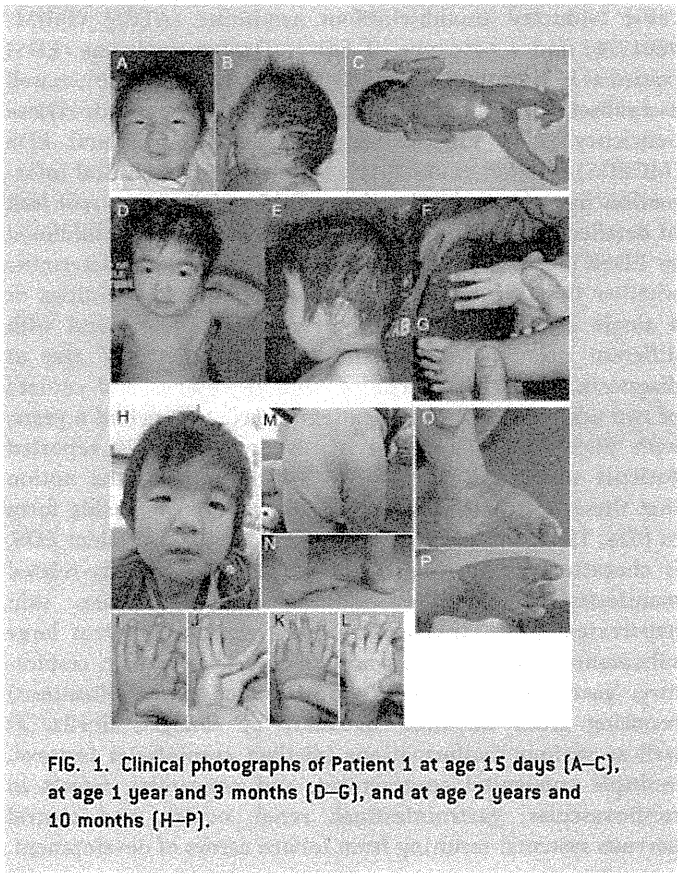

FIG. 1. Clinical photographs of Patient 1 at age 15 days (A–C), at age 1 year and 3 months (D–G), and at age 2 years and 10 months (H–P).

and buttocks after falling, which were absorbed spontaneously. Bleeding time was 1.3 min (normal values, 1–5 min), prothrombin time-international normalized ratio (PT-INR) 1.00 (normal values, 0.81–1.38 sec), and activated partial thromboplastin time (APTT) 27.9 sec (normal values, 23–36 sec).

When seen by us at age 1 year and 3 months, his craniofacial shape became square with a broad, bossed forehead, and hypertelorism with downslanting palpebral fissures became evident (Fig. 1D, E). Skin redundancy and tapering fingers and toes were noted (Fig. 1D, F, G). Ear rotation and flexion contractures of fingers improved (Fig. 1E, F).

When last seen by us at age 2 years and 10 months, he weighed 9.86 kg (−2.4 SD), height 84.9 cm (−2.1 SD), and OFC 45.5 cm (−2.4 SD). His face was slender, and was characterized by an unclosed fontanelle, hypertelorism, short and downslanting palpebral fissures, blue sclerae, strabismus, a short nose with a hypoplastic columella, low-set ears, a high palate, a long philtrum, a thin upper lip vermillion, a small mouth, and microretrognathia (Fig. 1H). He had a Marfanoid habitus, generalized joint laxity, a flat and thin thorax, and distinctive fingers (tapering with enlargement of distal phalanges) (Fig. 1I–L), and talipes valgus and planus with extremely soft subcutaneous tissues at the heels (Fig. 1N–P). The distal IP joints in bilateral index to little fingers and the IP/metacarpophalangeal (MP) joints in bilateral thumbs could hardly be flexed or extended. The MP joints in bilateral index to little fingers could be moved with poor flexion and hyperextension (see Supplementary Video 1 online). He had hyperextensible to redundant skin with bruisability and fine palmer creases (Fig. 1J, L, M). He suffered from constipation (defecation twice a week), treated with oral magnesium oxide. Ophthalmological examinations showed mild esotropia, and amblyopia due to severe hyperopic astigmatism. A cardiac ultrasonography showed no defects or valve abnormalities but mild dilation of the ascending aorta at the sinus of Valsalva. A brain CT showed no ventricular enlargement (Fig. 3O, P). G-banded chromosomes were normal. The Kinder Infant Developmental Scale [Cheng et al., 2010] showed mild developmental delay with the overall developmental quotient as 65 (physical/motor, 35; manipulation, 58; receptive language, 77; expressive language, 103; conceptual thinking, 77; social relationships with children, 68; social relationships with adults, 116; home training, 68; feeding, 42). He had orchiopexy and a surgical correction of an umbilical hernia at age 2 years and 7 months.

Patient 2

The patient, a Japanese boy, was the first child of a healthy 25-year-old mother and a healthy 28-year-old nonconsanguineous father. He was born by normal vaginal delivery at 38 weeks of gestation. His birth weight was 2940 g (+0.3 SD), length 49.1 cm (+0.3 SD), and OFC 32 cm (−0.5 SD). He was admitted for the treatment of bilateral adducted thumbs and talipes equinovarus. His craniofacial features included a large fontanelle, a high forehead, hypertelorism, short and downslanting palpebral fissures, blue sclerae, strabismus, a short nose with a hypoplastic columella, low-set and rotated ears, a high palate, a long philtrum, a thin upper lip vermillion, a small mouth, and microretrognathia (Fig. 2A). He had arachnodactyly, flexion-adduction contractures of bilateral thumbs, flexion contractures of the IP joints in the other fingers, rigidity of bilateral hip joints, and mild pectus excavatum (Fig. 2A, B). He also had widely spaced nipples, a redundant skin, and bilateral cryptorchidism (Fig. 2A). He suckled poorly and hated to be hugged tightly, suggesting hyperalgesia to pressure. Talipes equinovarus was treated with serial plaster casts. Gross motor development was delayed: He raised his head at 7 months, sat without support at age 1 year and 2 months, crawled at age 1 year and 6 months, pulled himself up by holding to something at age 1 year and 6 months, and walked unassisted at age 2 years and 6 months. His fontanelle was closed at age 3 years.

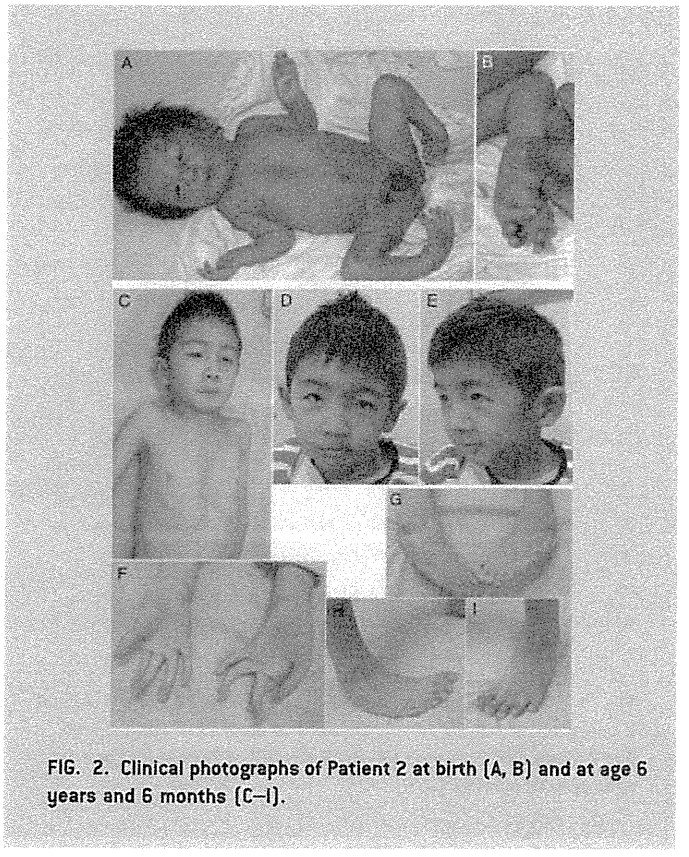

FIG. 2. Clinical photographs of Patient 2 at birth (A, B) and at age 6 years and 6 months (C–I).

At age 3 years, he developed a large subcutaneous hematoma over the skull after falling. Hematomas on the lower legs frequently occurred. He had recurrent dislocations of bilateral shoulders.

When last seen by us at age 6 years and 6 months, he weighed 16.4 kg (−1.4 SD), height 112 cm (−1.0 SD), and OFC 51.5 cm (−0.2 SD). He could jump unassisted. His craniofacial features included hypertelorism, short and downslanting palpebral fissures, blue sclerae, strabismus, a short nose with a hypoplastic columella, low-set ears, a high palate, a long philtrum, a thin upper lip vermillion, a small mouth, and microretrognathia (Fig. 2D, E). He had a Marfanoid habitus, generalized joint laxity, and pectus excavatum (Fig. 2C). His fingers were cylindrical and slender (Fig. 2F). He showed talipes equinovarus when lying down (Fig. 2G) and talipes planus when standing (Fig. 2H, I). The subcutaneous tissues at the heels were extremely soft. The distal IP joints in bilateral index to little fingers and the IP joints in bilateral thumbs